INTERNATIONAL JOURNAL OF
RADIATION ONCOLOGY • BIOLOGY • PHYSICS
www.redjournal.org

BIOLOGY CONTRIBUTION

Carbon Ion and Photon Radiation Therapy Show Enhanced Antitumoral Therapeutic Efficacy With Neoantigen RNA-LPX Vaccines in Preclinical Colon Carcinoma Models

Nadja Salomon, PhD,* Alexander Helm, PhD,† Abderaouf Selmi, PhD,* Claudia Fournier, PhD,† Mustafa Diken, PhD,* Barbara Schrörs, PhD,* Michael Scholz, PhD,† Sebastian Kreiter, MD,* Marco Durante, PhD,†,‡,§ and Fulvia Vascotto, PhD*

*TRON gGmbH, Translational Oncology at the University Medical Center of the Johannes Gutenberg University Mainz, Mainz, Germany; †GSI Helmholtzzentrum for Heavy Ion Research GmbH, Darmstadt, Germany; ‡Technical University Darmstadt, Institute of Condensed Matter Physics, Darmstadt, Germany; and §University Federico II, Department of Physics "Ettore Pancini", Naples, Italy

Received Aug 31, 2023; Accepted for publication Dec 27, 2023

Purpose: Personalized liposome-formulated mRNA vaccines (RNA-LPX) are a powerful new tool in cancer immunotherapy. In preclinical tumor models, RNA-LPX vaccines are known to achieve potent results when combined with conventional X-ray radiation therapy (XRT). Densely ionizing radiation used in carbon ion radiation therapy (CIRT) may induce distinct effects in combination with immunotherapy compared with sparsely ionizing X-rays.

Methods and Materials: Within this study, we investigate the potential of CIRT and isoeffective doses of XRT to mediate tumor growth inhibition and survival in murine colon adenocarcinoma models in conjunction with neoantigen (neoAg)-specific RNA-LPX vaccines encoding both major histocompatibility complex (MHC) class I– and class II–restricted tumor-specific neoantigens. We characterize tumor immune infiltrates and antigen-specific T cell responses by flow cytometry and interferon-γ enzyme-linked immunosorbent spot (ELISpot) analyses, respectively.

Results: NeoAg RNA-LPX vaccines significantly potentiate radiation therapy–mediated tumor growth inhibition. CIRT and XRT alone marginally prime neoAg-specific T cell responses detected in the tumors but not in the blood or spleens of mice. Infiltration and cytotoxicity of neoAg-specific T cells is strongly driven by RNA-LPX vaccines and is accompanied by reduced expression of the inhibitory markers PD-1 and Tim-3 on these cells. The neoAg RNA-LPX vaccine shows similar overall therapeutic efficacy in combination with both CIRT and XRT, even if the physical radiation dose is lower for carbon ions than for X-rays.

Conclusions: We hence conclude that the combination of CIRT and neoAg RNA-LPX vaccines is a promising strategy for the treatment of radioresistant tumors.

Corresponding authors: Fulvia Vascotto, PhD; and Nadja Salomon, PhD; E-mail: nadja.salomon@tron-mainz.de, fulvia.vascotto@tron-mainz.de

Funding: The carbon ion radiation therapy results presented here are based on the experiment SBIO_08_Salomon, which was performed at the SIS18 accelerator of the GSI Helmholtz Centre for Heavy Ion Research (Darmstadt, Germany) in the frame of FAIR Phase-0.

Data Sharing Statement: All data generated and analyzed during this study are included in this published article (and its supplementary information files).

Acknowledgments—We thank Y. Ahrberg, I. Beulshausen, M. Brkic, S. Linkenbach, U. Schmitt, M. Schork, J. Sriha, and C. Totis for technical assistance.

Supplementary material associated with this article can be found, in the online version, at doi:10.1016/j.ijrobp.2023.12.042.

https://doi.org/10.1016/j.ijrobp.2023.12.042

Introduction

Combined with different immunotherapies, high-dose radiation therapy primes antitumoral T cell responses that facilitate tumor regression at local and metastatic sites.[1] Recent preclinical findings suggest that not only classical photon or γ-ray radiation therapy can induce immune modulation and abscopal responses, but also particle radiation therapy.[2-5] Particles such as protons or heavy ions have favorable dose-depth profiles and deliver their highest dose near the end of their range in the so-called Bragg peak.[6] Hence, particle therapy is rapidly growing worldwide.

High-dose radiation therapy has both antigenicity and adjuvant function; that is, irradiation enhances the expression of major histocompatibility complex (MHC) class I on target cells, leads to the differential expression and peptide processing of tumor antigens,[7-9] and induces type I interferon (IFN) responses and recruitment of local antigen-presenting cells via the accumulation of double-stranded DNA and micronuclei in the cytoplasm.[10,11] These in situ vaccination effects are mostly inefficient after radiation alone and can be greatly enhanced after combination with antibodies against cytotoxic T lymphocyte−associated protein 4,[12] programmed cell death 1 (PD-1)/programmed cell death ligand 1 (PD-L1),[13,14] CD40,[14] and CD137,[15] immune modulators such as Fms-related tyrosine kinase 3 ligand,[16] interleukin-2,[17] granulocyte-macrophage colony-stimulating factor,[18] and therapeutic cancer vaccines.[19-21]

Heavy ion therapy has distinct biologic features compared with X-rays due to the densely ionizing deposition pattern in the target volume.[22] One of those features is tumor immune modulation; hence, it is of great interest to experimentally characterize the combination of carbon ion radiation therapy (CIRT) and different immunotherapies.[23,24]

Whereas immune-checkpoint inhibitors (ICIs) and other immunomodulatory agents, such as cytokines, act on pre-existing antitumoral T cell responses, therapeutic cancer vaccines induce de novo T cell responses and amplify and reinvigorate pre-existing T cell responses (reviewed in Lang et al[25]). Recent studies demonstrate the synergy between X-ray radiation therapy (XRT) and tumor antigen-specific RNA-LPX-based cancer vaccines[26] in preclinical models of HPV16$^+$ disease[19] and colon carcinoma.[20] Antigen-encoding RNA is engineered for optimized intracellular stability and translational efficiency[27-29], introducing special sequences, such as a 5′ cap, 5′ and 3′ untranslated regions, poly(A) tail; and for epitope presentation on MHC class I and II molecules[30], flanking the encoded antigen with a secretion signal and MHC class I transmembrane domain. Cancer vaccines based on this format are currently being tested in combination with antibodies against PD-1 in patients with HPV16$^+$ and PD-L1$^+$ head and neck squamous cell carcinoma and melanoma in several randomized phase 2 clinical trials (NCT04534205, NCT04526899, and NCT03815058).

Given the limitations of single-agent therapy, combination therapy is often superior in achieving local and systemic tumor control. In this study, we wanted to assess the therapeutic potential of CIRT and novel RNA-LPX−based cancer vaccines as a potential future immunotherapy treatment option in patients who classify for CIRT. As a second endpoint, we wanted to analyze if CIRT is superior to XRT regarding tumor immune modulation and T cell priming. To separate this from tumor control solely due to physical characteristics of CIRT versus XRT, we applied isoeffective instead of physical doses.

To this aim, we used the highly mutated murine MC38 colorectal carcinoma model[31] and applied neoantigen (neoAg)-specific RNA-LPX vaccines that encode the immunodominant MHC class I−restricted antigen Rpl18[32] and 10 in-house−identified MHC class II−restricted antigens.

Methods and Materials

Mice

Age-matched, female C57BL/6 wild-type mice were purchased from Envigo. The regulatory authorities for animal welfare approved the experimental group sizes and procedures. Mice were kept at the BioNTech SE and GSI Helmholtz Centre in accordance with federal and state policies on animal research.

Tumor cell lines

The murine C57BL/6 colorectal tumor cell line MC38 was provided by the Leiden University Medical Center. The murine BALB/c colorectal cancer cell line CT26 was purchased from ATCC (CRL-2638). The murine C57BL/6 HPV16 E6/E7$^+$ tumor cell line TC-1[33] was obtained from T. C. Wu (Johns Hopkins University). Master and working cell banks were generated immediately after receipt, and cells from the fifth to ninth passages were used for in vivo experiments.

Photon radiation therapy

XRT was performed with the orthovoltage X-ray source X-RAD320 (Precision X-Ray, Inc) at a dose rate of 0.93 Gy/min (cell lines) or 0.47 Gy/min (in vivo experiments). Tumors were unidirectionally irradiated from above, and mice were shielded with customized lead shields with a 20-mm−diameter aperture above the tumor.

CIRT

CIRT was performed at GSI Helmholtz Centre for Heavy Ion Research at the heavy ion synchrotron SIS18. Irradiation was delivered to tumors at 240 MeV/u and 40 mm spread-

out Bragg peak with a mean dose averaged linear energy transfer of 55 to 60 keV/μm (range shifter, bolus of 71-mm water-equivalent thickness). CIRT irradiation conditions were aligned with those of XRT, and mice were unidirectionally irradiated from above in an area with a diameter of 20 mm.

Clonogenic survival assay

Clonogenic survival of MC38 cells was assessed after XRT to determine the relative biologic effectiveness for the in vivo exposure of tumors to CIRT. Clonogenic survival was assessed using the standard colony-forming assay described elsewhere.[34,35] In 2 independent experiments, MC38 tumor cells were seeded into 25-cm^2 tissue culture flasks in triplicate and irradiated 2 days later with different doses of XRT (0-10 Gy). Cell were incubated for 7 days and fixed and stained with methylene blue solution (30% Loeffler's methylene blue plus 5% methanol; Sigma-Aldrich), and cell clusters of at least 50 cells were counted. The local effect model[36,37] was used to estimate the dose-effect curve for CIRT and the carbon beam relative biologic effectiveness (Fig. E2). As displayed in Figure E2b, 2 Gy XRT is as biologically effective as 1 Gy CIRT, 4 Gy XRT is as biologically effective as 2 Gy CIRT, 6 Gy XRT is as biologically effective as 4 Gy CIRT, 8 Gy XRT is as biologically effective as 6 Gy CIRT, and 10 Gy XRT is as biologically effective as 8 Gy CIRT.

Mutation selection

For mutation detection, RNA and whole-exome sequencing of MC38 tumor cells and C57BL/6 tissue samples were performed by TRON gGmbH, and somatic single-nucleotide variants (SNVs) and short insertions/deletions were identified as described previously.[31] A previously identified MHC class I−restricted epitope derived from an SNV in Rpl18 (Rpl18$_{Q125R}$)[32] and 10 in-house−identified MHC class II−restricted epitopes (sequencing, expression analysis and mutation calling as described in Schrörs et al[31]) were selected for neoAg RNA-LPX vaccines. MHC class II epitopes were chosen based on strong MHC class II−binding prediction (IEDB v2.13, method "consensus3") and high RNA expression levels (data not shown).

Plasmid RNA constructs and in vitro transcription

Plasmid templates for in vitro transcription of neoAg-encoding RNAs were generated, cloning the MHC class I −restricted epitope Rpl18 and 10 in-house−identified MHC class II−restricted epitopes, each for fusion with MHC class I transmembrane and cytoplasmic domains.[26,28,30,38] Mutated amino acids were encoded as 27 mers with SNVs at position 14.[39] Rpl18 was cloned as a monotope and the 10 above indicated MHC class II−restricted epitopes as a decatope fused to each other by 10-amino acid−long glycine-serine linkers. Both antigen-encoding vectors were in vitro transcribed and capped with the β-S antireverse cap analog.[29] For neoAg RNA-LPX vaccination, both antigen-encoding RNAs were pooled. The same vector backbone without an antigen-encoding open reading frame was used as control RNA.

RNA-LPX preparation

RNA-LPX vaccines were generated as previously described.[20,26]

Synthetic peptides

Synthetic peptides were synthetized by JPT Peptide Technologies at a purity above 90% for the MHC class I −restricted epitope Rpl18 (9 mer, KILTFDRL) and for 4 of the best-predicted MHC class II−restricted epitopes (27 mer, SNV at position 14).

Tumor models and treatment

C57BL/6 mice were subcutaneously injected with 5×10^5 MC38 tumor cells into the right flank, and tumor growth was measured unblinded with a caliper every 2 to 3 days. Tumor volumes were calculated by $(a^2 \times b)/2$ (where a is the width, and b is the length). Mice were randomized according to tumor size before treatment and immunized intravenously with 20 μg of neoAg each composed of 10 μg of Rpl18 mRNA and 10 μg of MHC class II−restricted decatope mRNA or control RNA-LPX vaccine. Tumor-bearing mice were irradiated with isoeffective doses, that is, either 12 Gy XRT or 10 Gy CIRT, as described above. Isoeffective doses were calculated for MC38 tumors based on MC38 clonogenic cell survival assays. Tumor irradiation was performed under ketamine/xylazine (CIRT) or isoflurane (XRT) narcosis. The termination criteria included a tumor volume of >1500 mm^3, more than 20% body weight loss compared to the start of the experiment, severe tumor necrosis (dry defect with >25% surface area, wet defect with a cavity greater than one-third of the tumor height or chronically wet defect), or other signs of severe illness.

Tissue preparation

Tumor single-cell suspensions were generated using a mouse tumor dissociation kit and gentleMACS dissociator (both Miltenyi Biotec) according to manufacturer's instructions. Spleen single-cell suspensions were generated as previously described.[38] CD4/CD8 tumor-infiltrating lymphocyte

magnetic-activated cell sorting (TIL MACS; Miltenyi Biotec) was performed according to manufacturer's instructions.

Flow cytometry

Flow cytometry staining was performed on cell lines, full blood, and tumor and spleen single-cell suspensions. Cells were stained with viability dyes (eBioscience) according to manufacturer's instructions. For extracellular staining, anti-mouse CD45, CD4, CD44, CD40L CD25, NK1.1, PD-L1, cleaved caspase-3 (CC3; BD Pharmingen), CD8α (clone 5H10), PD-1 (Invitrogen), T cell immunoglobulin and mucin domain-3 (TIM-3), H-2 (pan−MHC class I; BioLegend), and KLRG1 (eBioscience) antibodies were used. For intracellular and intranuclear staining, anti-mouse IFNγ (Invitrogen), tumor necrosis factor-α (TNFα), Foxp3 (BD Pharmingen), and thymocyte selection−associated HMG BOX (TOX; Miltenyi) antibodies were used. Rpl18-specific $CD8^+$ T cells were stained with custom-made Rpl18 (KILTFDRL) H2-K^b−restricted tetramers (MBL). For CC3, IFNγ, and TNFα staining, samples were fixed and permeabilized with Cytofix/Cytoperm (BD Pharmingen). Foxp3 and TOX staining was performed using a Foxp3 fixation kit (eBioscience) according to manufacturer's instructions. Intracellular cytokine staining was performed as described previously,[40] and CD4/CD8 TILs (TIL MACS) were stimulated with 2 μg/mL MHC class I peptide−loaded C57BL/6 bone marrow−derived dendritic cells in the presence of 10 μg/mL Brefeldin A (Sigma) for 5 hours at 37°C. Peripheral blood was stained with Rpl18 MHC dextramers as previously described.[38] Immune cell populations were gated as previously described,[19] and Rpl18-specific $CD8^+$ T cells were identified as $CD45^+CD8^+$Rpl18 $multimer^+KLRG1^+$. Flow cytometric data were acquired on an LSR Fortessa (BD Biosciences) and analyzed using FlowJo 10.8,

IFNγ enzyme-linked immunospot (ELISpot) assays

ELISpot assays were performed as previously described[41] by incubating 5×10^5 splenocytes with 5×10^4 MC38 tumor cells, 2 μg/mL MHC class I− or 4 μg/mL MHC class II −restricted peptides overnight at 37°C. All samples were tested in duplicate.

High-mobility group protein 1 (HMGB1) enzyme-linked immunosorbent assays (ELISA)

Cell culture supernatants were collected 72 hours after irradiation exposure and stored at −80°C. For assessment of HMGB1 concentrations, the HMGB1 Express ELISA (IBL) was used according to the manufacturer's instructions. Supernatants were diluted 1:25 for MC38 and 1:3.3 for CT26 and TC-1.

Statistical analyses and data presentation

Data are presented as mean ± standard error of the mean. Statistical analyses were performed using GraphPad PRISM 9, and comparisons were considered statistically significant when the P value was less than 0.05 ($^*P \leq 0.05$, $^{**}P \leq 0.01$, and $^{***}P \leq 0.001$). Specific statistical analyses of each experiment are described in the corresponding figure legends.

Results

CIRT is superior to XRT regarding cell death induction and tumor immune modulation in murine tumor cell lines

First, we wanted to characterize the cytotoxic and immunomodulatory potential of XRT and CIRT in murine MC38 (Fig. 1), CT26, and TC-1 tumor cell lines (Fig. E1). In comparison to untreated cells, 3 days after irradiation, the fraction of harvested cells was strongly reduced by XRT as well as CIRT in a dose-dependent manner (Fig. 1a, Fig. E1a, h). When assessing the live cell fraction and the induction of the apoptosis marker CC3, CIRT was more cytotoxic than XRT at the same physical doses applied in all 3 cell lines (Fig. 1b, c, and Fig. E1b, c, i, j).

The immunomodulatory potential of CIRT versus XRT was analyzed by staining cells with antibodies against MHC class I (pan-H2), the inhibitory receptor PD-L1, and the immunogenic cell death marker ecto-calreticulin and by measuring HMGB1 secreted protein in the supernatant[42] (Fig. 1d-g, Fig. E1d-f, k-m). MHC class I was robustly upregulated by CIRT up to 4 Gy in MC38 tumor cells, whereas higher doses of CIRT did not lead to an additional increase nor did any dose of XRT (Fig. 1d). A similar observation was made in TC-1 tumor cells, whereas CT26 tumor cells were also sensitive to XRT and responded with MHC class I upregulation (Fig. E1d, k). PD-L1 expression was increased in a dose-dependent manner in MC38 tumor cells after CIRT, whereas XRT did not modulate PD-L1 above 2 Gy (Fig. 1e). In CT26 and TC-1 tumor cells, PD-L1 expression reached a plateau at >2 Gy CIRT as well as XRT (Fig. E1e, l). Ecto-calreticulin expression dose-dependently increased in CIRT-treated, but not XRT-treated, MC38 tumor cells (Fig. 1f), whereas no significant difference was observed in TC-1 and CT26 tumor cells (Fig. 1f, m). HMGB1 secretion was detected in the supernatants of MC38, CT26, and TC-1 tumor cells, with a strong dose dependency and with CIRT mediating more release than XRT in all cell lines (Fig. 1g, Fig. E1g, n).

In line with previous reports,[2] CIRT and XRT mediated distinct immunologic effects with similar trends observed in all cell lines tested. As MC38 tumor cells responded with a higher effectivity of CIRT in all conditions, they were chosen for further in vivo experiments.

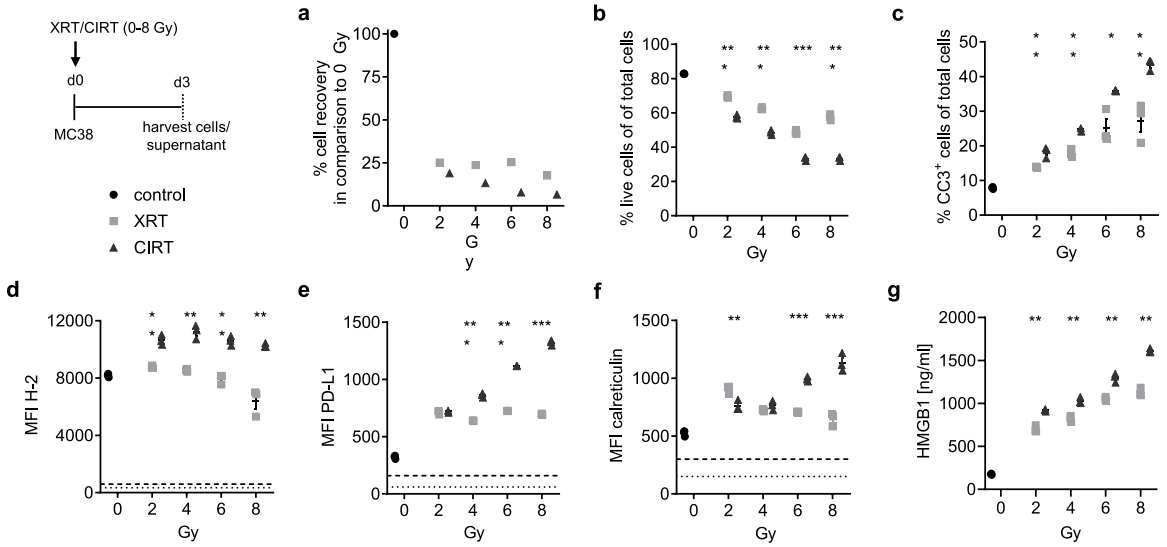

Fig. 1. Carbon ion radiation therapy (CIRT) is superior to X-ray radiation therapy (XRT) regarding cell death induction and tumor immune modulation in MC38 murine tumor cell lines.
MC38 murine tumor cell lines were irradiated with different doses of XRT and CIRT (0-8 Gy) and analyzed 3 days later for (a) fraction of harvested cells compared with untreated cells (0 Gy), (b-f) the percentage and expression of different markers, as evaluated by flow cytometry, and (g) the concentration of HMGB1 in the supernatant, as determined by enzyme-linked immunosorbent assay. (b-f) Flow cytometry analysis of (b) the percentage of live cells, (c) the percentage of $CC3^+$ cells, and (d-f) the median fluorescence intensity (MFI) of (d) H-2, (e) PD-L1, and (f) ecto-calreticulin. Significance was determined using 2-tailed *t* tests. Dashed lines indicate the median fluorescence intensity of unstained (fine)- and isotype (bold)-stained cells.

RNA-LPX neoAg vaccination synergizes equivalently with CIRT or XRT to restrict MC38 tumor growth

Whereas radiation therapy can sensitize the tumor for killing by specific cytotoxic $CD8^+$ T cells,[19] $CD4^+$ T cells in turn can enhance radiation therapy—mediated in situ priming.[20] To potentially account for both mechanisms, in the present study, we evaluated the therapeutic efficacy of CIRT and neoAg RNA-LPX vaccines encoding both MHC class I − and class II—restricted neoAg. MC38 tumor-bearing mice were immunized with neoAg RNA-LPX vaccine on days 7, 13, and 21 and were locally irradiated with either 12 Gy XRT or an isoeffective dose of 10 Gy CIRT on day 16 (average tumor volume of ~90 mm^3; Fig. 2). An RNA-LPX molecule that contains all structural features of the mRNA (5′cap, 5′ untranslated region, MHC class I trafficking domain, secretion signal, 3′ untranslated region, and poly (A) tail) but does not encode an antigen was used as a control for neoAg RNA-LPX—treated mice. NeoAg-specific RNA-LPX vaccines alone already induced tumor growth inhibition (Fig. 2a, Fig. E3a) compared with the control RNA-LPX vaccine. Both irradiation modalities, XRT and CIRT, facilitated tumor growth inhibition from the day of radiation therapy to approximately 10 days after, when tumors stared to regrow again (Fig. 2a, Fig. E3a). The therapeutic effects of CIRT and XRT were enhanced by combined neoAg-specific vaccination, and both irradiation modalities were equally effective. Mouse survival data are displayed in Figure E3b; however, as many mice had to be euthanized before reaching the endpoint of 1500 mm^3 in this tumor model because of critical necrosis, these data did not serve to discriminate survival therapeutic effects as well as the tumor growth data did (Fig. 2a, Fig. E3a). T cell responses against the immunodominant MC38 antigen Rpl18[32] were monitored in the blood 10 days after the last vaccination (Fig. 2b). As expected, the neoAg-specific RNA-LPX vaccine, which encodes Rpl18 as 1 of the vaccine antigens, generated a high frequency of Rpl18-specific $CD8^+$ T cells (~20% of total $CD8^+$ T cells) that were almost undetectable in control or CIRT/XRT monotherapy—treated mice. After combination with CIRT and XRT, neoAg-induced Rpl18-specific $CD8^+$ T cells were slightly, but not significantly, enhanced (~30% of total $CD8^+$ T cells), an effect that could be attributed to additional tumor antigen release and T cell priming by radiation therapy.

Despite a lower physical dose was applied, CIRT was as effective as XRT in tumor growth inhibition and synergized with neoAg-specific RNA-LPX vaccines. Neither therapy alone was able to reject MC38 tumors, a fact that is attributed to the initiation of therapy in rather advanced tumors.

NeoAg RNA-LPX mediates tumor immune infiltration

Next, we aimed to characterize cellular drivers responsible for the enhanced efficacy of combination therapy and

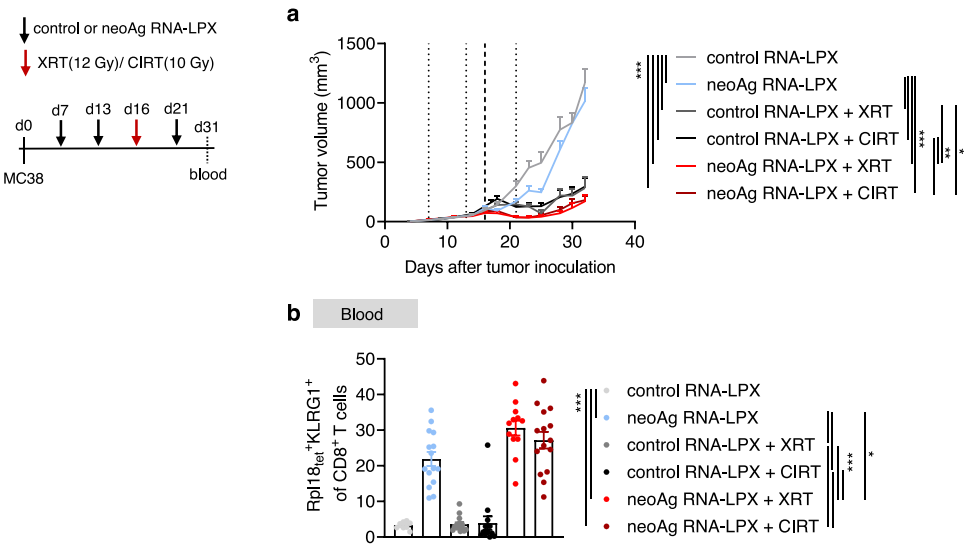

Fig. 2. RNA-LPX neoantigen vaccination synergizes equivalently with carbon ion radiation therapy (CIRT) and X-ray radiation therapy (XRT) to restrict MC38 tumor growth.
MC38 tumor-bearing C57BL/6 mice were treated as indicated. (a) Tumor volume was monitored over time (n = 21-22 mice/group) and is displayed up to day 32, the last time point at which >30% of control group mice were still alive. Treatments are indicated as fine (RNA-LPX) and bold (radiation therapy) dashed lines. (b) Rpl18-specific $CD8^+$ T cells in the blood on day 31 (n = 8-15 mice/group). Significance was determined using (a) 2-way analysis of variance and Tukey's multiple comparison test and (b) 1-way analysis of variance and Tukey's multiple comparison test. To account for missing values of deceased mice in tumor growth analyses, the last observation (tumor volume) was carried forward[54] until day 32.

excised tumors at a time point at which intragroup differences were strongest (day 26; Fig. 2a). Tumor single-cell suspensions were generated, and infiltrating immune cells (Fig. 3a-d) and their expression of inhibitory receptors (Fig. 3e, f) were analyzed by flow cytometry. Compared with control RNA-LPX–treated mice, neoAg-specific RNA-LPX vaccines enhanced total leukocyte infiltration, as did combination therapy, but not radiation therapy alone (Fig. 3a, left). The total tumor cell fraction remained unchanged by XRT and was only marginally reduced by CIRT (Fig. 3a, right), which can be attributed to the time point chosen (10 days after radiation therapy), at which tumors start to regrow (Fig. 2a). Infiltration of total $CD8^+$ T cells, $CD4^+$ T cells, and natural killer (NK) cells was significantly enhanced in CIRT/neoAg RNA-LPX–treated mice, whereas all other treatment groups failed to strongly modulate these immune subsets (Fig. 3b). Regulatory T cells were moderately enriched in XRT/neoAg RNA-LPX–treated mice but not in CIRT/neoAg RNA-LPX–treated mice.

Intratumoral, immunodominant Rpl18-specific $CD8^+$ T cells were significantly expanded by neoAg RNA-LPX vaccines (~50% of total $CD8^+$ T cells) but also after XRT (~25%) and CIRT (~40%) monotherapy (Fig. 3c). Combined radiation therapy did not further magnify neoAg RNA-LPX vaccine–induced Rpl18-specific $CD8^+$ T cell responses. Neoantigen-specific $CD4^+$ T cells were present in neoAg RNA-LPX–vaccinated mice but not in XRT- or CIRT-treated mice (Fig. 3d). The expression of the inhibitory markers PD-1 and Tim-3 and the transcription factor TOX, a transcriptional and epigenetic regulator of cell exhaustion,[43] on $CD8^+$ T cells was highest in XRT- and CIRT-treated mice and was reversed after combined neoAg-specific vaccination (Fig. 3e). Within the $CD4^+$ T cell subset, PD-1 and Tim-3 expression was significantly lowered, especially in CIRT/neoAg RNA-LPX–treated mice (Fig. 3f).

Interestingly, tumors of CIRT/neoAg RNA-LPX–treated mice were strongly infiltrated with total and antigen-specific $CD8^+$ and $CD4^+$ T cells and NK cells and displayed low expression of the inhibitory markers PD-1 and Tim-3 on $CD8^+$ T cells as well as $CD4^+$ T cells. For XRT/neoAg RNA-LPX–treated mice, a similar picture emerged; however, NK cell infiltration was not enhanced, nor was the expression of inhibitory markers reduced on $CD4^+$ T cells.

Antigen-specific immune responses are mainly primed by neoAg RNA-LPX

To examine if combined CIRT and neoAg-specific RNA-LPX vaccines hold the potential to reduce secondary or metastatic tumors, systemic (splenic) T cell responses were analyzed against MC38 tumor cells and MC38 immunodominant MHC class I– and class II–restricted neoAg by IFNγ ELISpot (Fig. 4a). T cell responses directed at MC38 tumor cells were amplified in neoAg RNA-LPX–vaccinated mice and were largely directed against the immunodominant MHC class I–restricted antigen Rpl18 (Fig. 4a, left and middle). $CD8^+$ T cell responses were

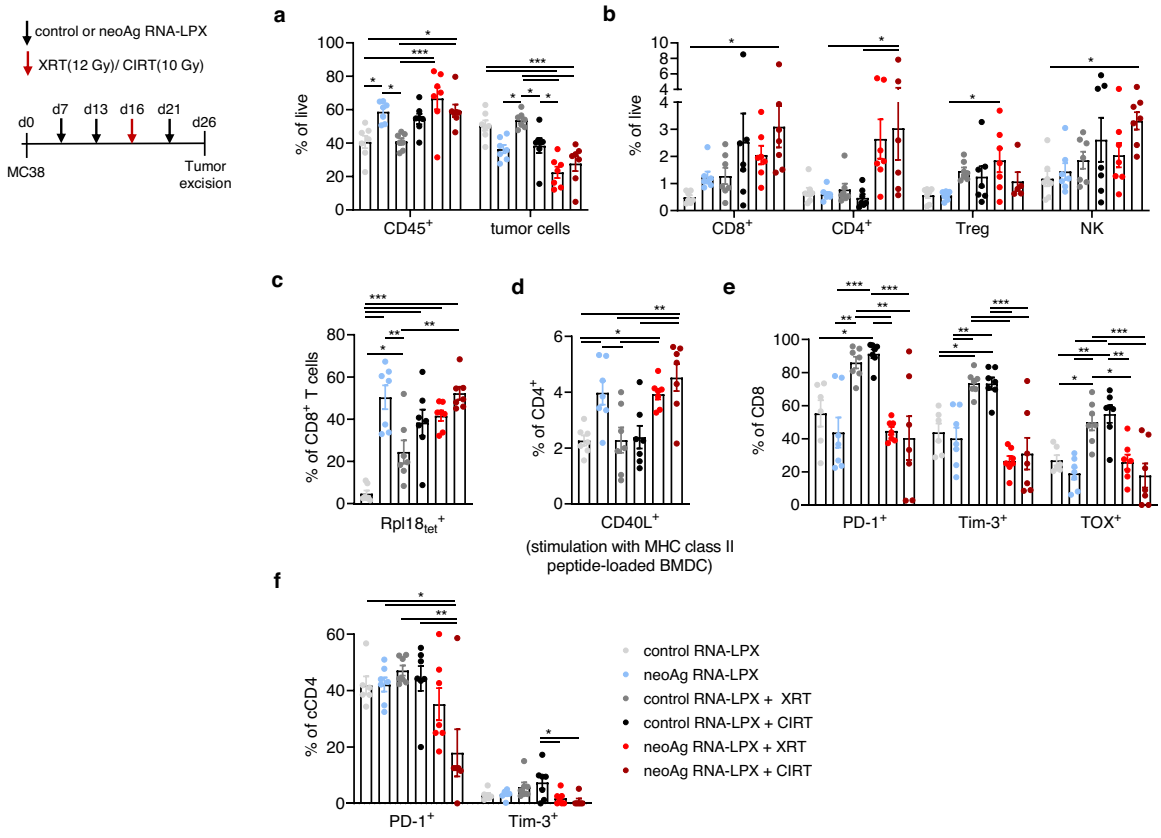

Fig. 3. Neoantigen (neoAg) RNA-LPX mediates tumor immune cell infiltration.
MC38 tumor-bearing C57BL/6 mice were treated as indicated. Tumors were excised on day 26, single-cell suspensions were generated, and cell composition was evaluated by flow cytometry. The percentages of $CD45^+$ leukocytes (a, left), tumor cells (a, right), tumor-infiltrating $CD8^+$ T cells (b, left), $CD4^+$ T cells (b, middle left), regulatory T cells (T_{reg}; b, middle right), and natural killer cells (NK; b, right) out of the total number of live cells are shown. (c) Percentage of $Rpl18_{tet}^+$ cells out of $CD8^+$ T cells. (d) Percentage of $CD40L^+$ cells out of $CD4^+$ T cells. For CD40L staining, tumor samples were restimulated ex vivo with major histocompatibility complex (MHC) class II peptide–loaded bone marrow–derived dendritic cells. (e and f) Percentage of (e) PD-1^+, Tim-3^+, and TOX^+ cells within $CD8^+$ T cells, and (f) PD-1^+ and Tim-3^+ cells within $CD4^+$ T cells. Significance in a to f was determined using 1-way analysis of variance and Tukey's multiple comparison test.

slightly, but not significantly, enhanced in XRT- and CIRT-treated mice, indicating basal levels of T cell priming by both radiation modalities. Neoantigen-specific $CD4^+$ T cell responses were solely detected in groups vaccinated with those neoantigens and not in XRT- or CRT-treated mice (Fig. 4a, right). Whereas CIRT lead to a slightly higher infiltration of Rpl18-specific $CD8^+$ T cells than XRT (Fig. 3c) but not significantly, the effector function of $CD8^+$ T cells remained the same 10 days after radiation therapy (Fig. 4a, left and middle), indicating a similar priming efficacy of CIRT and XRT.

Apart from the total number of T cells primed, the effector function and cytotoxic potential of T cells are potential predictors of secondary tumor rejection. Thus, intratumoral T cells were stimulated with immunodominant Rpl18 antigens, and IFNγ and TNFα expression was analyzed (Fig. 4b). NeoAg RNA-LPX–vaccinated mice harbored the largest fraction of IFNγ- and TNFα-producing $CD8^+$ T cells, whether they were irradiated or not. CIRT or XRT alone failed to produce a significant amount of IFNγ and TNFα expression in Rpl18-specific $CD8^+$ T cells (Fig. 4b), which is in line with the finding of generally low $CD8^+$ T cell priming in these treatment groups.

In summary, antitumoral T cell responses were mainly driven by neoAg RNA-LPX vaccines; however, CIRT and XRT monotherapy also minimally primed tumor-specific T cells.

Discussion

To our knowledge, this is the first study combining CIRT and neoAg-specific cancer vaccines. Our data suggest an enhanced therapeutic efficacy of CIRT or XRT and neoAg-specific RNA-LPX vaccines in MC38 tumor model, with antitumoral effects exceeding those of either monotherapy. A dose of 10 Gy CIRT was equally effective as 12 Gy XRT in mediating local tumor growth inhibition and T cell priming,

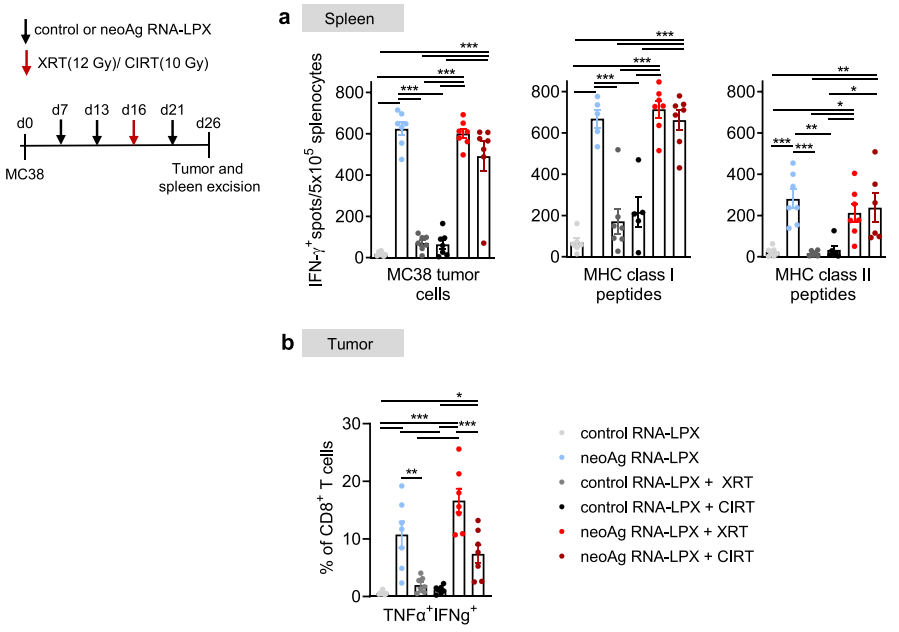

Fig. 4. Antigen-specific immune responses are mainly primed by neoantigen (neoAg) RNA-LPX.
MC38 tumor-bearing C57BL/6 mice were treated as indicated in Figure 3. Tumors and spleens were excised on day 26, and single-cell suspensions were generated for the analysis of (a) splenocytes by interferon-γ (IFNγ) enzyme-linked immunospot and (b) tumors by flow cytometry. (a) IFNγ^+ spots detected after incubation of whole splenocytes with MC38 tumor cells (left), major histocompatibility complex (MHC) class I (middle), and MHC class II (right) peptides. (b) Flow cytometry staining of IFNγ and tumor necrosis factor-α (TNFα) in intratumoral CD8$^+$ T cells after restimulation with Rpl18 peptides. Significance was determined using One-way analysis of variance and Tukey's multiple comparison tests.

both as a monotherapy and in combination with neoAg RNA-LPX vaccines.

At the same physical doses used, CIRT exerted a higher cytotoxic and more pronounced tumor-immune modulation on MC38 murine tumor cell lines than XRT, which is in line with previous reports.[2] Expression of MHC class I and ecto-calreticulin, and HMGB1 secretion were significantly upregulated in CIRT-treated MC38 cells compared with in XRT-treated MC38 cells, as was PD-L1 expression. Similar results were observed for CT26 and TC-1 cell lines but with less clear differences between CIRT and XRT regarding PD-L1 and ecto-calreticulin expression. Hence, CIRT not only possesses an enhanced biologic effectiveness in cell death induction but also tumor immune modulation.

Tumors of CIRT/neoAg RNA-LPX− and XRT/neoAg RNA-LPX−treated mice were heavily infiltrated with neoAg-specific T cells that displayed reduced expression of the inhibitory markers PD-1 and Tim-3 and high IFNγ and TNFα cytokine secretion. These antitumoral T cell responses were mainly driven by neoAg RNA-LPX vaccines, as CIRT and XRT monotherapy−treated tumors were less immune infiltrated with high expression of the inhibitory markers PD-1 and Tim-3 and lacked inflammatory cytokine secretion. Combined neoAg RNA-LPX/CIRT−treated mice were the only mice that demonstrated significantly enhanced NK infiltration over control RNA-LPX−vaccinated mice. Enhanced NK cell infiltration was also observed in CIRT-treated E0771 murine tumors.[44] As reported previously, enhanced NK cell infiltration could be attributed to radiation-induced CXCL16 release from tumor cells and CXCR6 surface expression on NK cells.[45] As we did not observe therapeutic benefits over XRT/neoAg RNA-LPX−treated mice, it is an open question whether enhanced NK infiltration translates to enhanced antitumoral responses.

Whereas ICIs expand T cells from pre-existing T cell responses, cancer vaccines prime T cell responses towards a de novo antigenic source, which makes them attractive for minimally T cell−inflamed tumors. Cancer vaccines are not restricted to mutated, personalized neoantigens, such as SNVs,[46] insertions/deletions, or fusion genes,[25] but can also encode nonmutated tumor-associated antigens[47]. As cancer vaccines already induce systemic T cell responses, the investigation of radiation therapy−mediated "abscopal" responses is rendered difficult. Within this study, we did not implant secondary tumors and instead followed peripheral Rpl18 antigen-specific cytotoxic CD8$^+$ T cell responses, the population that should be the principal driver of antitumoral responses in secondary tumors. High amounts of Rpl18-specific CD8$^+$ T cell responses were readily induced by neoAg RNA-LPX vaccines, whereas CIRT and XRT only marginally primed antigen-specific immune responses compared with control groups. It was previously demonstrated that radiation therapy in situ priming could be enhanced not only after combination with ICIs[12-14] but also after

vaccination with MHC class II–restricted tumor neoantigens.[20] MHC class II–restricted neoantigens were also encoded on neoAg vaccine vectors, but as they also encoded immunodominant MHC class I–restricted Rpl18, in situ priming effects might have been masked in an already saturated Rpl18-specific $CD8^+$ T cell response.

According to the Particle Therapy Cooperative Group database, around 46,000 cancer patients have been treated with CIRT in 14 centers across 6 different countries[48] CIRT has proven to be safe and effective across many different cancer types, such as brain, prostate, lung, and head and neck cancer.[49] Whereas most ongoing clinical trials focus on dose-escalating schedules of CIRT against classical XRT, a small number of trials are assessing CIRT and immunotherapy combinations, such as NCT02946138 (a phase 2 trial of CIRT [40 Gy/5 fractions] and granulocyte-macrophage colony-stimulating factor in hepatocellular carcinoma),[50] NCT05229614 (a phase 2 trial of CIRT and ICIs in different cancers with disease stability after pembrolizumab),[51] and NCT04143984 (a phase 2 trial of CIRT and camrelizumab [anti-PD-1] in patients with locally recurrent nasopharyngeal carcinoma). Especially when combining radiation therapy and immunotherapy approaches, off-target cytotoxic effects on circulating and intratumoral immune cell populations should be taken into account. Due to a different dose-depth distribution, CIRT spares circulating lymphocytes to a greater extent than conventional XRT while preserving dose conformity on the tumor,[52] which makes it even more attractive for combination with immunotherapies such as cancer vaccines. The benefits of CIRT were not fully exploited in this study, as, for a direct comparison of both radiation modalities, irradiation angles and windows were matched with those of less advanced XRT machines. Accordingly, isoeffective doses with respect to clonogenic cell survival were chosen for better comparison and clinical transferability. In fact, both tumor control and immunologic endpoints were generally comparable, despite few differences between XRT and CIRT in some endpoints.

Due to the negative net charge, RNA-LPX formulations directly target mRNA to antigen-presenting cells in lymphoid organs, mainly the spleen.[26] Depending on the type of formulation, other peptide- or mRNA-based cancer vaccines might use other routes of administration, such as intranodal or intramuscular injection.[53] The ultimate and shared goal of different vaccine formats is the targeting of antigen-presenting cells at high amounts, with potent innate immune stimulation (self-adjuvant or external adjuvant), high antigen translation and stability, and the selection of highly immunogenic tumor-specific antigens.

The data presented here provide insight into what needs to be considered for the combination of cancer vaccines and CIRT in a clinical setting. Whereas CIRT is technologically more advanced in abrogating tumor cell clonogenic survival while sparing healthy tissues, cancer vaccines mobilize tumor-specific T cell responses. Two sides of the medal are needed for efficient tumor eradication.

References

1. Ngwa W, Irabor OC, Schoenfeld JD, Hesser J, Demaria S, Formenti SC. Using immunotherapy to boost the abscopal effect. *Nat Rev Cancer* 2018;18:313-322.
2. Hartmann L, Schröter P, Osen W, et al. Photon versus carbon ion irradiation: Immunomodulatory effects exerted on murine tumor cell lines. *Sci Rep* 2020;10:21517.
3. Gameiro SR, Malamas AS, Bernstein MB, et al. Tumor cells surviving exposure to proton or photon radiation share a common immunogenic modulation signature, rendering them more sensitive to T cell-mediated killing. *Int J Radiat Oncol Biol Phys* 2016;95:120-130.
4. Helm A, Tinganelli W, Simoniello P, et al. Reduction of lung metastases in a mouse osteosarcoma model treated with carbon ions and immune checkpoint inhibitors. *Int J Radiat Oncol Biol Phys* 2021;109:594-602.
5. Ando K, Fujita H, Hosoi A, et al. Intravenous dendritic cell administration enhances suppression of lung metastasis induced by carbon-ion irradiation. *J Radiat Res* 2017;58:446-455.
6. Durante M, Paganetti H. Nuclear physics in particle therapy: A review. *Rep Prog Phys* 2016;79:96702.
7. Reits EA, Hodge JW, Herberts CA, et al. Radiation modulates the peptide repertoire, enhances MHC class I expression, and induces successful antitumor immunotherapy. *J Exp Med* 2006;203:1259-1271.
8. Sharma A, Bode B, Wenger RH, et al. γ-Radiation promotes immunological recognition of cancer cells through increased expression of cancer-testis antigens in vitro and in vivo. *PLoS ONE* 2011;6:e28217.
9. Gameiro SR, Jammeh ML, Wattenberg MM, Tsang KY, Ferrone S, Hodge JW. Radiation-induced immunogenic modulation of tumor enhances antigen processing and calreticulin exposure, resulting in enhanced T-cell killing. *Oncotarget* 2014;5:403-416.
10. Harding SM, Benci JL, Irianto J, Discher DE, Minn AJ, Greenberg RA. Mitotic progression following DNA damage enables pattern recognition within micronuclei. *Nature* 2017;548:466-470.
11. Deng L, Liang H, Xu M, et al. STING-dependent cytosolic DNA sensing promotes radiation-induced type I interferon-dependent antitumor immunity in immunogenic tumors. *Immunity* 2014;41:843-852.
12. Formenti SC, Rudqvist N-P, Golden E, et al. Radiotherapy induces responses of lung cancer to CTLA-4 blockade. *Nat Med* 2018;24:1845-1851.
13. Deng L, Liang H, Burnette B, et al. Irradiation and anti-PD-L1 treatment synergistically promote antitumor immunity in mice. *J Clin Invest* 2014;124:687-695.
14. Honeychurch J, Glennie MJ, Johnson PWM, Illidge TM. Anti-CD40 monoclonal antibody therapy in combination with irradiation results in a CD8 T-cell-dependent immunity to B-cell lymphoma. *Blood* 2003;102:1449-1457.
15. Rodriguez-Ruiz ME, Rodriguez I, Garasa S, et al. Abscopal effects of radiotherapy are enhanced by combined immunostimulatory mAbs and are dependent on CD8 T cells and crosspriming. *Cancer Res* 2016;76:5994-6005.
16. Demaria S, Ng B, Devitt ML, et al. Ionizing radiation inhibition of distant untreated tumors (abscopal effect) is immune mediated. *Int J Radiat Oncol Biol Phys* 2004;58:862-870.
17. Yasuda K, Nirei T, Tsuno NH, Nagawa H, Kitayama J. Intratumoral injection of interleukin-2 augments the local and abscopal effects of radiotherapy in murine rectal cancer. *Cancer Sci* 2011;102:1257-1263.
18. Golden EB, Chhabra A, Chachoua A, et al. Local radiotherapy and granulocyte-macrophage colony-stimulating factor to generate abscopal responses in patients with metastatic solid tumours: A proof-of-principle trial. *Lancet Oncol* 2015;16:795-803.
19. Salomon N, Selmi A, Grunwitz C, et al. Local radiotherapy and E7 RNA-LPX vaccination show enhanced therapeutic efficacy in preclinical models of $HPV16^+$ cancer. *Cancer Immunol Immunother* 2022;71:1975-1988.
20. Salomon N, Vascotto F, Selmi A, et al. A liposomal RNA vaccine inducing neoantigen-specific $CD4^+$ T cells augments the antitumor

activity of local radiotherapy in mice. *Oncoimmunology* 2020;9 1771925.
21. Zheng W, Skowron KB, Namm JP, et al. Combination of radiotherapy and vaccination overcomes checkpoint blockade resistance. *Oncotarget* 2016;7:43039-43051.
22. Durante M, Debus J, Loeffler JS. Physics and biomedical challenges of cancer therapy with accelerated heavy ions. *Nat Rev Phys* 2021;3:777-790.
23. Helm A, Totis C, Durante M, Fournier C. Are charged particles a good match for combination with immunotherapy? Current knowledge and perspectives. *Int Rev Cell Mol Biol* 2023;376:1-36.
24. Helm A, Fournier C, Durante M. Particle radiotherapy and molecular therapies: Mechanisms and strategies towards clinical applications. *Expert Rev Mol Med* 2022;24 109370.
25. Lang F, Schrörs B, Löwer M, Türeci Ö, Sahin U. Identification of neoantigens for individualized therapeutic cancer vaccines. *Nat Rev Drug Discov* 2022;21:261-282.
26. Kranz LM, Diken M, Haas H, et al. Systemic RNA delivery to dendritic cells exploits antiviral defence for cancer immunotherapy. *Nature* 2016;534:396-401.
27. Orlandini von Niessen AG, Poleganov MA, Rechner C, et al. Improving mRNA-based therapeutic gene delivery by expression-augmenting 3′ UTRs identified by cellular library screening. *Mol Ther* 2019;27:824-836.
28. Holtkamp S, Kreiter S, Selmi A, et al. Modification of antigen-encoding RNA increases stability, translational efficacy, and T-cell stimulatory capacity of dendritic cells. *Blood* 2006;108:4009-4017.
29. Kuhn AN, Diken M, Kreiter S, et al. Phosphorothioate cap analogs increase stability and translational efficiency of RNA vaccines in immature dendritic cells and induce superior immune responses in vivo. *Gene Ther* 2010;17:961-971.
30. Kreiter S, Selmi A, Diken M, et al. Increased antigen presentation efficiency by coupling antigens to MHC class I trafficking signals. *J Immunol* 2008;180:309-318.
31. Schrörs B, Hos BJ, Yildiz IG, et al. MC38 colorectal tumor cell lines from two different sources display substantial differences in transcriptome, mutanome and neoantigen expression. *Front Immunol* 2023;14 1102282.
32. Hos BJ, Camps MGM, van den Bulk J, et al. Identification of a neo-epitope dominating endogenous CD8 T cell responses to MC-38 colorectal cancer. *Oncoimmunology* 2019;9 1673125.
33. Lin KY, Guarnieri FG, Staveley-O'Carroll KF, et al. Treatment of established tumors with a novel vaccine that enhances major histocompatibility class II presentation of tumor antigen. *Cancer Res* 1996;56:21-26.
34. Fournier C, Scholz M, Weyrather WK, Rodemann HP, Kraft G. Changes of fibrosis-related parameters after high- and low-LET irradiation of fibroblasts. *Int J Radiat Biol* 2009;77:713-722.
35. Weyrather WK, Ritter S, Scholz M, Kraft G. RBE for carbon track-segment irradiation in cell lines of differing repair capacity. *Int J Radiat Biol* 2009;75:1357-1364.
36. Elsässer T, Weyrather WK, Friedrich T, et al. Quantification of the relative biological effectiveness for ion beam radiotherapy: Direct experimental comparison of proton and carbon ion beams and a novel approach for treatment planning. *Int J Radiat Oncol Biol Phys* 2010; 78:1177-1183.
37. Friedrich T, Scholz U, Elsässer T, Durante M, Scholz M. Calculation of the biological effects of ion beams based on the microscopic spatial damage distribution pattern. *Int J Radiat Biol* 2011;88:103-107.
38. Grunwitz C, Salomon N, Vascotto F, et al. HPV16 RNA-LPX vaccine mediates complete regression of aggressively growing HPV-positive mouse tumors and establishes protective T cell memory. *Oncoimmunology* 2019;8 e1629259.
39. Kreiter S, Vormehr M, van de Roemer N, et al. Mutant MHC class II epitopes drive therapeutic immune responses to cancer. *Nature* 2015; 520:692-696.
40. Diken M, Vormehr M, Grunwitz C, Kreiter S, Türeci Ö, Sahin U. Discovery and subtyping of neo-epitope specific T-cell responses for cancer immunotherapy: Addressing the mutanome. *Methods Mol Biol* 2017;1499:223-236.
41. Kreiter S, Selmi A, Diken M, et al. Intranodal vaccination with naked antigen-encoding RNA elicits potent prophylactic and therapeutic antitumoral immunity. *Cancer Res* 2010;70:9031-9040.
42. Yamazaki T, Hannani D, Poirier-Colame V, et al. Defective immunogenic cell death of HMGB1-deficient tumors: Compensatory therapy with TLR4 agonists. *Cell Death Differ* 2014;21:69-78.
43. Khan O, Giles JR, McDonald S, et al. TOX transcriptionally and epigenetically programs $CD8^+$ T cell exhaustion. *Nature* 2019;571:211-218.
44. Hartmann L, Osen W, Eichmüller OL, et al. Carbon ion irradiation plus CTLA4 blockade elicits therapeutic immune responses in a murine tumor model. *Cancer Lett* 2022;550 215928.
45. Yoon MS, Pham CT, Phan M-TT, et al. Irradiation of breast cancer cells enhances CXCL16 ligand expression and induces the migration of natural killer cells expressing the CXCR6 receptor. *Cytotherapy* 2016;18:1532-1542.
46. Sahin U, Derhovanessian E, Miller M, et al. Personalized RNA mutanome vaccines mobilize poly-specific therapeutic immunity against cancer. *Nature* 2017;547:222-226.
47. Sahin U, Oehm P, Derhovanessian E, et al. An RNA vaccine drives immunity in checkpoint-inhibitor-treated melanoma. *Nature* 2020;585:107-112.
48. Particle Therapy Co-Operative Group. Particle therapy facilities in clinical operation. Available at: https://ptcog.site/index.php/facilities-in-operation-public. Accessed April 13, 2023.
49. Durante M, Orecchia R, Loeffler JS. Charged-particle therapy in cancer: Clinical uses and future perspectives. *Nat Rev Clin Oncol* 2017;14:483-495.
50. Lazar AA, Schulte R, Faddegon B, Blakely EA, Roach III M. Clinical trials involving carbon-ion radiation therapy and the path forward. *Cancer* 2018;124:4467-4476.
51. Cavalieri S, Vitolo V, Barcellini A, et al. Immune checkpoint inhibitors and carbon iON radiotherapy in solid cancers with stable disease (ICONIC). *Future Oncol* 2023;19:193-203.
52. Durante M, Formenti S. Harnessing radiation to improve immunotherapy: Better with particles? *Br J Radiol* 2020;93 20190224.
53. Beck JD, Reidenbach D, Salomon N, et al. mRNA therapeutics in cancer immunotherapy. *Mol Cancer* 2021;20:69.
54. Overall JE, Tonidandel S, Starbuck RR. Last-observation-carried-forward (LOCF) and tests for difference in mean rates of change in controlled repeated measurements designs with dropouts. *Social Sci Res* 2009;38:492-503.